Efficiency and Droop Improvement in InGaN/GaN Light-Emitting Diodes by Selective Carrier Distribution Manipulation

2012 Appl. Phys. Express 5 042101

(http://iopscience.iop.org/1882-0786/5/4/042101)

Applied Physics Express **5** (2012) 042101
DOI: 10.1143/APEX.5.042101

Efficiency and Droop Improvement in InGaN/GaN Light-Emitting Diodes by Selective Carrier Distribution Manipulation

Chao-Hsun Wang, Shih-Pang Chang, Pu-Hsi Ku, Yu-Pin Lan, Chien-Chung Lin[1],
Hao-Chung Kuo*, Tien-Chang Lu, Shing-Chung Wang, and Chun-Yen Chang[2]

Department of Photonics and Institute of Electro-Optical Engineering, National Chiao Tung University, Hsinchu, Taiwan 30010, R.O.C.
[1] *Institute of Photonic Systems, College of Photonics, National Chiao-Tung University, Guiren Township, Tainan, Taiwan 71150, R.O.C.*
[2] *Institute of Electronics, National Chiao-Tung University, Hsinchu, Taiwan 30010, R.O.C.*

Received February 6, 2012; accepted March 1, 2012; published online March 16, 2012

Efficiency and droop behavior in InGaN/GaN light-emitting diodes (LEDs) are both improved using selectively graded composition multiple quantum barriers (SGQBs). Simulation results show that SGQBs could moderately improve the hole transport in the active region. In the meantime, the spatial distribution overlap between electrons and holes in the active region could also be well considered. Therefore, the radiative recombination of the SGQB LED is more efficient than that of the conventional LED. The overall efficiency and droop behavior are simultaneously improved in the SGQB LED, at both low and high current densities.

GaN-based light-emitting diodes (LEDs) are the most potential candidates for next-generation illumination sources due to their high lumen efficiency, compact size, and long lifetime.[1)] One key issue that still needs to be solved is the so-called "efficiency droop". After a five-year-long debate, the major mechanisms for droop could be considered as electron overflow out of the active region, insufficient transport of holes, and Auger recombination.[2–4)] Among these factors, improving the hole transport was identified as a breakthrough for the alleviation of efficiency droop. Poor hole transport could lead to the accumulation of these carriers at the quantum wells near p-GaN, which increase the possibilities for the overflow of electrons and Auger recombination at a high carrier concentration. Various designs such as coupled multiple quantum wells (MQWs),[5)] multi-layered barriers,[6)] and graded-well-thickness structure[7)] were reported and proved to be effective.

In our previous work, we demonstrated that leveling the triangular barriers at the valance band by graded-composition multi-quantum barriers (GQBs) from $\mathrm{In}_x\mathrm{Ga}_{1-x}\mathrm{N}$ to GaN along the [0001] direction could effectively enhance the hole transport in the active region.[8)] The results showed a uniform hole distribution and low efficiency droop (only 6%). However, most of the works involving the improvement in the hole transport in the active region have a fatal disadvantage, that is their efficiencies are relatively low at standard-operation current density, around 20 to 40 A/cm^2, as compared with their reference samples.[5,6,8)] This phenomenon has greatly limited the feasibility of improving the droop behavior, because the LEDs nowadays are still operated at low current density. One of the reasons for this drawback could be attributed to the poor spatial distribution between electrons and holes.[8)]

In this paper, we report an optimal design for barriers in MQWs by selectively grading the composition of barriers from $\mathrm{In}_x\mathrm{Ga}_{1-x}\mathrm{N}$ to GaN along [0001] direction, to form selectively graded composition multiple quantum barriers (SGQBs) and show the appropriate improvement in the transport of holes in the active region. The simulation results show that selectively improving the hole transport has a better impact on the efficiency and droop behavior than thoroughly improving it.

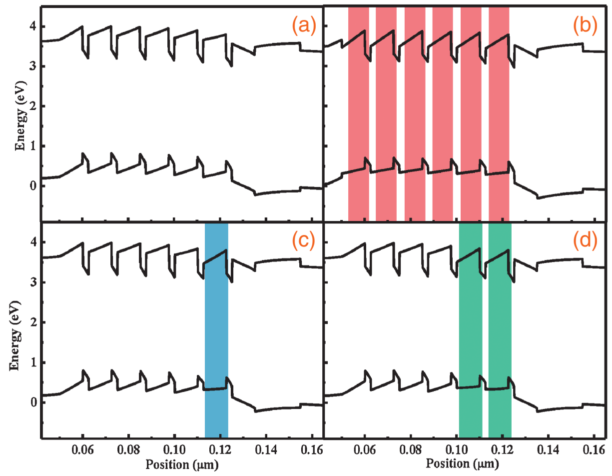

Fig. 1. Calculated band diagrams of (a) conventional LED, (b) LED I with all its barriers graded, (c) LED II with its fifth barrier graded, and (d) LED III with its fourth and fifth barriers graded at 100 A/cm^2.

The LED structures were simulated using APSYS simulation software, which was developed by Crosslight Software.[9)] The conventional LED structure was composed of a 100-μm-thick c-plane sapphire substrate, a 4-μm-thick n-type GaN layer (n-doping $= 2 \times 10^{18}$ cm^{-3}), six pairs of $\mathrm{In}_{0.15}\mathrm{Ga}_{0.85}\mathrm{N}/\mathrm{GaN}$ MQWs with 2.5-nm-thick wells and 10-nm-thick barriers, a 20-nm-thick p-$\mathrm{Al}_{0.15}\mathrm{Ga}_{0.85}\mathrm{N}$ electron blocking layer (p-doping $= 5 \times 10^{17}$ cm^{-3}), and a 200-nm-thick p-type GaN layer (p-doping $= 1 \times 10^{18}$ cm^{-3}). For comparison, we have three types of LEDs with different designs, namely 1) all the multiple quantum barriers (MQBs) are graded with indium composition from 5 to 0% along the [0001] direction, noted as LED I; 2) only the fifth barrier is graded, noted as LED II; 3) the fourth and fifth barriers are graded, noted as LED III, as shown in Fig. 1. The barriers with graded composition could level the triangular barriers at the valance band, which was reported to be beneficial to the hole transport.[8)] Commonly accepted physical parameters were adopted to perform the simulations: percentage of screening effect of 50%, Shockley–Read–Hall recombination lifetime of 1 ns, and Auger recombination coefficient in quantum wells on the order of 10^{-31} cm^6/s, respectively.[10)] Other material parameters used in the simulation

---

*E-mail address: hckuo@faculty.nctu.edu.tw

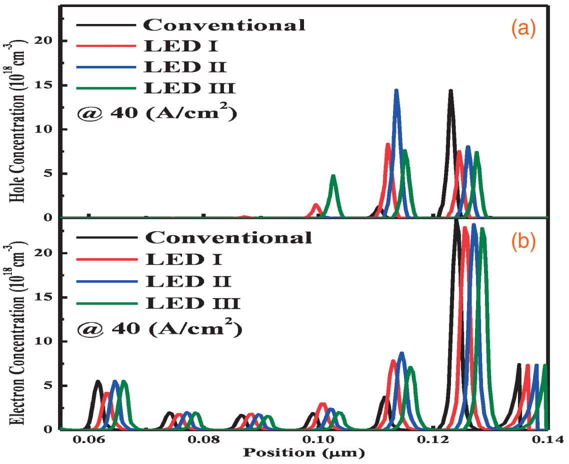

Fig. 2. (a) Hole concentrations and (b) electron concentrations of conventional LED, LED I, LED II, and LED III at 40 A/cm^2.

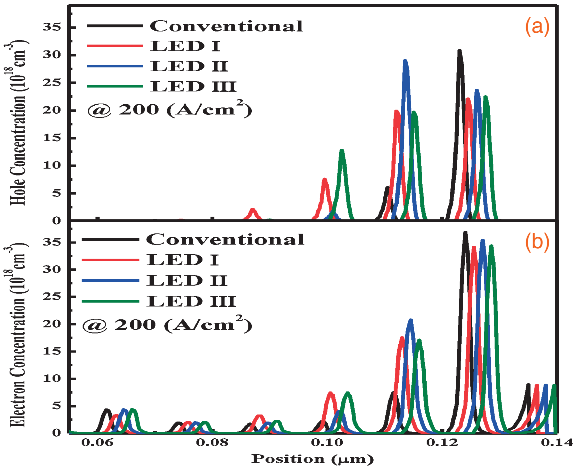

Fig. 3. (a) Hole concentrations and (b) electron concentrations of conventional LED, LED I, LED II, and LED III at 200 A/cm^2.

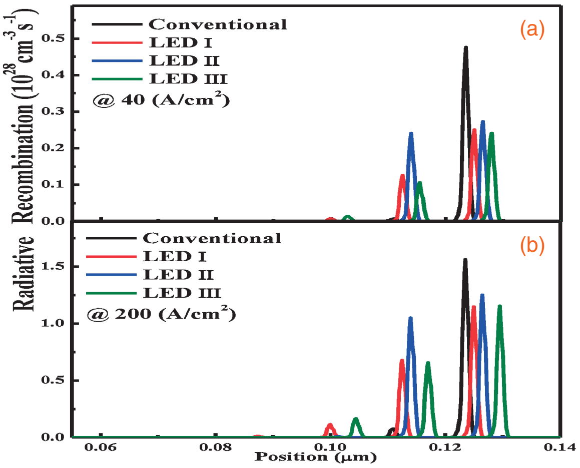

Fig. 4. Radiative recombination distributions of conventional LED, LED I, LED II, and LED III at (a) 40 A/cm^2 and (b) 200 A/cm^2.

can be found in ref. 11. The LED has a typical chip size of 300 × 300 μm^2.

Figure 2 shows the calculated hole and electron distributions of the conventional LED and LEDs I, II, and III at the current density of 40 A/cm^2. The hole distribution of the conventional LED exhibits serious accumulation at the last well, which reveals the difficulty of hole transport in conventional structure. For LEDs I, II, and III with their fifth barriers graded, the holes at the last well are released to the previous wells. Subsequently, the holes are distributed more uniformly with more graded barriers. On the other hand, the electron distributions in Fig. 2(b) are slightly affected by the hole distribution, and most of the electrons are still located at the last well. The carrier distributions of the conventional LED and LEDs I, II, and III at the current density of 200 A/cm^2 show similar behaviors as those of 40 A/cm^2, as shown in Figs. 3(a) and 3(b). The holes and electrons are mostly located at the last three wells.

It is difficult to directly quantify the spatial overlap of holes and electrons because it has to include the wave function overlap of every well. However, we could still infer that information from the total radiative recombination. The radiative recombination distributions of the conventional LED, LED I, LED II, and LED III are shown in Fig. 4. For the conventional LED, the holes and electrons accumulate at the last well at low and high current densities, so does the radiative recombination. For LEDs I, II, and III, the carriers in the last well are released to the previous wells, and with more graded barriers, the holes are more uniformly distributed. The radiative recombination distributions are highly related to the hole distribution. However, these graded barriers have less effect on electron transport, so the electrons still mostly accumulated at the last well, as shown in Figs. 2(b) and 3(b). For LEDs I and III which have superior hole transport, the radiative recombination shows a certain amount at the fourth well, but the total radiative recombination is less than those of the conventional LED and LED II at low current density. The total radiative recombinations of LED I are 82 and 120% of those of the conventional LED at 40 and 200 A/cm^2, respectively. This phenomenon is quite common in other droop-reduction methods related to improving the hole transport.[12] On the hand, LED II shows 7 and 42% enhancements in total radiative recombination compared with those of the conventional LED. For the LED structures with six-pair MQWs, the radiative recombination mostly occurs at the last two wells. Even if the hole transport is thoroughly enhanced, the radiative recombination is still low due to the poor spatial overlap between holes and electrons. For LED II with its fifth barrier graded, the carriers radiatively recombined well in the last two wells, which give appropriate consideration to both hole transport and radiative recombination. Moreover, the simulation results also indicate that LED I has relatively smaller peak-wavelength-shift due to the enhanced hole transport. On the other hand, LED II has similar wavelength-shift behavior to the conventional one because its primary emission is still from the last two wells.

Figures 5(a) and 5(b) show the light output power and relative external quantum efficiency (EQE) as a function of current density for the LEDs with various MQB designs. It can be clearly seen that LEDs with more than two graded barriers (LEDs I and III) have superior droop behavior. The

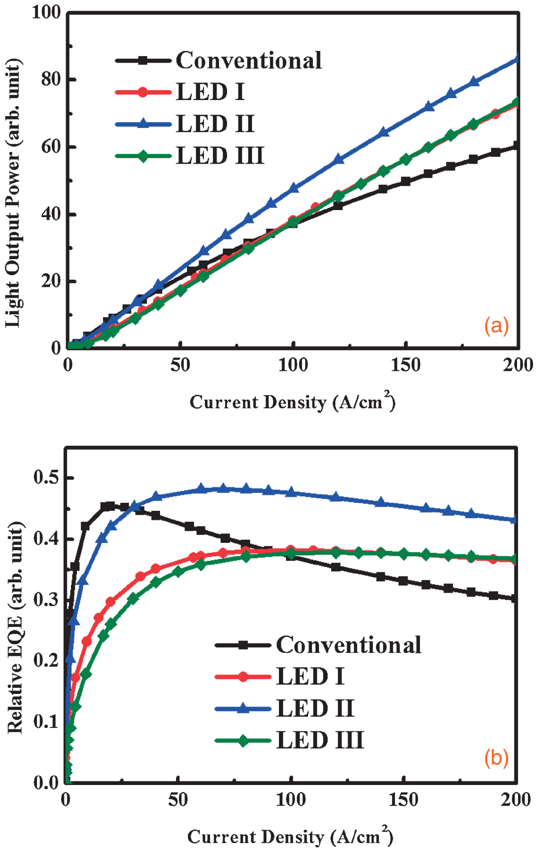

Fig. 5. Simulated (a) light output power and (b) relative EQE as functions of current density for conventional LED, LED I, LED II, and LED III.

light output powers of LEDs I and III are enhanced by 20% at 200 A/cm^2, as compared with that of the conventional LED. The efficiency droop behaviors, defined as ($\mathrm{EQE}_{\mathrm{peak}} - \mathrm{EQE}_{200\mathrm{A/cm}^2})/\mathrm{EQE}_{\mathrm{peak}}$, are only 6% or less in LEDs I and III, which are much smaller than that in the conventional LED (34%). However, these two LEDs have a lower EQE at standard-operation current density than the conventional one, which is not feasible for application even though their droop behavior is quite small. These results indicate that excessive improvement in hole transport is not practically helpful. For LED II with its fifth barrier graded, the light output power is enhanced by 7 and 42% compared with the conventional LED at 40 and 200 A/cm^2, respectively. Moreover, the efficiency droop behavior in LED II is 10%. This result shows that with moderate improvement in the hole transport in LED II, the enhancement of light output power occurs not only at a high current density of 200 A/cm^2, but also at a standard operation current density of 40 A/cm^2. On the other hand, the efficiency droop could be simultaneously reduced.

In conclusion, InGaN/GaN LEDs with selectively graded composition multiple quantum barriers were numerically investigated. The simulation results indicate that thoroughly improving the hole transport is helpful for the reduction of droop behavior, but not to the enhancement in radiative recombination due to the poor spatial overlap between holes and electrons. Therefore, selective carrier distribution manipulation was proposed and obtained using SGQBs. The SGQB LED with its fifth barrier graded shows improvements in both droop behavior and radiative recombination. The light output power of SGQB LED is enhanced by 7 and 42% at 40 and 200 A/cm^2, respectively. Moreover, the efficiency droop behavior is reduced from 34% in the conventional LED to 10% in SGQB LED. This work indicates that moderate improvement in the hole transport results in more efficient radiative recombination than thorough improvement, which is also more practical for lighting application.

Acknowledgment This work was funded by the National Science Council of Taiwan under grant number NSC 100-3113-E-009-001-CC2.

---

1) S. Pimputkar, J. S. Speck, S. P. DenBaars, and S. Nakamura: Nat. Photonics **3** (2009) 180.
2) M. H. Kim, M. F. Schubert, Q. Dai, J. K. Kim, E. F. Schubert, J. Piprek, and Y. Park: Appl. Phys. Lett. **91** (2007) 183507.
3) C. H. Wang, J. R. Chen, C. H. Chiu, H. C. Kuo, Y. L. Li, T. C. Lu, and S. C. Wang: IEEE Photonics Technol. Lett. **22** (2010) 236.
4) K. Ding, Y. P. Zeng, X. C. Wei, Z. C. Li, J. X. Wang, H. X. Lu, P. P. Cong, X. Y. Yi, G. H. Wang, and J. M. Li: Appl. Phys. B **97** (2009) 465.
5) X. Ni, Q. Fan, R. Shimada, Ü. Özgür, and H. Morkoç: Appl. Phys. Lett. **93** (2008) 171113.
6) Y. K. Kuo, T. H. Wang, J. Y. Chang, and M. C. Tsai: Appl. Phys. Lett. **99** (2011) 091107.
7) C. H. Wang, S. P. Chang, W. T. Chang, J. C. Li, Y. S. Lu, Z. Y. Li, H. C. Yang, H. C. Kuo, T. C. Lu, and S. C. Wang: Appl. Phys. Lett. **97** (2010) 181101.
8) C. H. Wang, S. P. Chang, P. H. Ku, J. C. Li, Y. P. Lan, C. C. Lin, H. C. Yang, H. C. Kuo, T. C. Lu, S. C. Wang, and C. Y. Chang: Appl. Phys. Lett. **99** (2011) 171106.
9) APSYS by Crosslight Software Inc., Burnaby, Canada.
10) Piprek: *Nitride Semiconductor Devices: Principles and Simulation* (Wiley-VCH, Weinheim, 2007), p. 279.
11) I. Vurgaftman and J. R. Meyer: J. Appl. Phys. **94** (2003) 3675.
12) D. Zhu, A. N. Noemaun, M. F. Schubert, J. Cho, E. F. Schubert, M. H. Crawford, and D. D. Koleske: Appl. Phys. Lett. **96** (2010) 121110.